Geosci. Model Dev. Discuss., https://doi.org/10.5194/gmd-2017-233
Manuscript under review for journal Geosci. Model Dev.
Discussion started: 2 November 2017

Geoscientific Model Development Discussions

The Bern Simple Climate Model (BernSCM) v1.0: an extensible and fully documented open source reimplementation of the Bern reduced form model for global carbon cycle-climate simulations

Kuno Strassmann[1,2] and Fortunat Joos[1]

[1]University of Bern, Switzerland
[2]now at Federal Institute of Technology, Switzerland

Correspondence to: Kuno Strassmann (kuno.strassmann@alumni.ethz.ch)

Abstract. The Bern Simple Climate Model (BernSCM) is a free open source reimplementation of a reduced form carbon cycle-climate model which has been used widely in previous scientific work and IPCC assessments. BernSCM represents the carbon cycle and climate system with a small set of equations for the heat and carbon budget, the parametrization of major nonlinearities, and the substitution of complex component systems with impulse response functions (IRF). The IRF approach allows cost-efficient yet accurate substitution of detailed parent models of climate system components with near linear behaviour. Illustrative simulations of scenarios from previous multi-model studies show that BernSCM is broadly representative of the range of the climate-carbon cycle response simulated by more complex and detailed models. Model code (in Fortran) was written from scratch with transparency and extensibility in mind, and is provided as open source. BernSCM makes scientifically sound carbon cycle-climate modeling available for many applications. Supporting up to decadal timesteps with high accuracy, it is suitable for studies with high computational load, and for coupling with, e.g., Integrated Assessment Models (IAM). Further applications include climate risk assessment in a business, public, or educational context, and the estimation of CO_2 and climate benefits of emission mitigation options.

1 Introduction

Simple climate models (SCM) consist of a small number of equations, which describe the climate system in an spatially and temporally highly aggregated form. SCMs have been used since the pioneering days of computational climate science, to analyse the planetary heat balance (Budyko, 1969; Sellers, 1969), and to clarify the role of the ocean and land compartments in the climate response to anthropogenic forcing through carbon and heat uptake (e.g., Oeschger et al., 1975; Siegenthaler and Oeschger, 1984; Hansen et al., 1984). Due to their modest computational demands, SCMs enabled pioneering research using the limited computational resources of the time, and continue to play a useful role in the hierarchy of climate models today.

Recent applications of SCMs are often found in research where computational resources are still limiting. Examples include probabilistic or optimization studies involving a large number of simulations, or the use of a climate component as part of a detailed interdisciplinary model. SCMs are also much easier to understand and handle than large climate models, which makes them useful as practical tools that can be used by non-climate experts for applications where detailed spatio-temporal physical

Geosci. Model Dev. Discuss., https://doi.org/10.5194/gmd-2017-233
Manuscript under review for journal Geosci. Model Dev.
Discussion started: 2 November 2017

modeling is not essential. This applies to interdisciplinary research, educational applications, or the quantification of the impact of emission reductions on climate change.

An important application of SCMs is in Integrated Assessment Models (IAMs). IAMs are interdisciplinary models that couple a climate component with an energy-economy model, to simulate emissions and their climate consequences. The comprehensive scope and sweeping interdisciplinarity of such models raise the challenge of maintaining a high and balanced scientific standard across all model components, especially when human resources are limited. This may apply particularly to the climate component, as IAMs are mostly used within the economic and engineering disciplines. Climate and carbon cycle representation are central parts of an IAM and have been critically assessed in the literature (Joos et al., 1999; Schultz and Kasting, 1997; Vuuren et al., 2009).

BernSCM is a zero-dimensional global carbon cycle-climate model built around impulse-response representations of the ocean and land compartments, as described previously in Joos et al. (1996); Joos and Bruno (1996); Meyer et al. (1999). The linear response of more complex ocean and land biosphere models with detailed process descriptions is captured using impulse-response functions (IRFs). These IRF-based substitute models are combined with nonlinear parametrizations of carbon uptake by the surface ocean and the terrestrial biosphere as a function of atmospheric CO_2 concentration and global mean surface temperature. Pulse response models have been shown to accurately emulate spatially resolved, complex models (Joos et al., 1996; Joos and Bruno, 1996; Meyer et al., 1999; Joos et al., 2001; Hooss et al., 2001).

The present version 1.0 of BernSCM is fundamentally analogous to the Bern Model as used already in the IPCC Second Assessment Report, Bern-SAR (whereas different versions of the Bern model family were used in the more recent IPCC reports). BernSCM represents the relevant processes more completely than Bern-SAR, thanks to additional alternative representations of the land and ocean components, which contain a more complete set of relevant sensitivities to temperature and atmospheric CO_2.

Here, BernSCM model simulations are compared to previous multimodel studies. The model is run for an idealized atmospheric pulse CO_2 emission experiment of Joos et al. (2013), and for the SRES A2 emission scenario used in the C4MIP study (Friedlingstein et al., 2006).

Together with this publication, BernSCM v1.0 is provided as an open source Fortran code for free use. The code was also rewritten from scratch, with flexibility and transparency in mind. The model is comprehensively documented, and easily extensible. New alternative model components can be added using the existing ones as a template. A range of numerical solution schemes is implemented. Up to decadal timesteps are supported with high accuracy, suitable for the coupling with, e.g., emission models of coarse time resolution. However, the published code is a ready-to-run standalone model which may also be useful in its own right.

BernSCM offers a physically sound carbon cycle-climate representation, but it is small enough for use in IAMs and other computationally tasking applications. In particular, the support of long time steps is ideally suited to the application of BernSCM a an IAM component, as these complex models often use time steps on the order of 10 years.

BernSCM also offers a tool to realistically assess the climate impact of carbon emissions or emission reductions and sinks, for example in aviation, forestry (Landry et al., 2016), blue carbon managment, peat development (Mathijssen et al., 2017), life

Geosci. Model Dev. Discuss., https://doi.org/10.5194/gmd-2017-233
Manuscript under review for journal Geosci. Model Dev.
Discussion started: 2 November 2017

Geoscientific Model Development Discussions

cycle assessments(Levasseur et al., 2016), or to assess the interaction of climate engineering interventions such as terrestrial carbon dioxide removal with the natural carbon cycle (Heck et al., 2016).

In this paper, we describe the model equations (section 2 and appendix A), uncertainty assessment (section 3), illustrative simulations in comparison with previous multi-model studies (section 4), followed by a discussion (section 5) and conlusions (section 6).

2 The BernSCM model framework and equations

BernSCM simulates the relation between CO_2 emissions, atmospheric CO_2, radiative forcing (RF), and global mean Surface Air Temperature (SAT) by budgeting carbon and heat fluxes globally between the atmosphere, the (abiotic) ocean, and the land biosphere compartments. Given CO_2 emissions and non-CO_2 RF, the model solves for atmospheric CO_2 and SAT (e.g., in the examples of section 4), but can also solve for carbon emissions (or residual uptake) when atmospheric CO_2 (or SAT and non-CO_2 RF) is prescribed, or for RF when SAT is prescribed.

The transport of carbon and heat to the deep ocean, as well as the decay of land carbon result from complex, but essentially linear behaviour of the ocean and land compartments. These are represented in BernSCM using impulse response functions (IRF, or Green's function). The IRF describes the evolution of a system variable after an initial perturbation, e.g., the pulse-like addition of carbon to a reservoir. It fully captures linear dynamics without representing the underlying physical processes (Joos et al., 1996). More illustratively, the model can be considered to consist of box models, which are an equivalent representation of the IRF model components (Figure 1).

The net primary production (NPP) of the land biosphere and the surface ocean carbon uptake depend on atmospheric CO_2 and surface temperature in a nonlinear way. These essential nonlinearities are described by parametrizations linking the linear model components.

2.1 Carbon cycle component

The budget equation for carbon is

$$\frac{\mathrm{d}m_A}{\mathrm{d}t} = e - f_O - \frac{\mathrm{d}m_L}{\mathrm{d}t} \tag{1}$$

where m_A denotes the atmospheric carbon stored in CO_2, e denotes CO_2 emissions, f_O the flux to the ocean, m_L the land biosphere carbon stock, and t is time. Here, m_L refers to the (potential) natural biosphere. Human impacts on the land biosphere exchange (LULUC) are not simulated in the present version, and treated as exogenous emissions (e). An overview of the model variables and parameters is given in tables 1 and 2.

The change in land carbon is given by the balance of net primary production (NPP) and decay of assimilated terrestrial carbon,

$$\frac{\mathrm{d}m_L}{\mathrm{d}t} = f_{\mathrm{NPP}} - f_{\mathrm{decay}} \tag{2}$$

Geosci. Model Dev. Discuss., https://doi.org/10.5194/gmd-2017-233
Manuscript under review for journal Geosci. Model Dev.
Discussion started: 2 November 2017

Decay includes heterotrophic respiration (RH), fire and other disturbances due to natural processes.

Carbon is taken up by the ocean through the air-sea interface (f_O) and distributed to the mixed surface layer (m_S) and the deep ocean interior (f_{deep})

$$f_O = \frac{\mathrm{d}m_S}{\mathrm{d}t} + f_{\mathrm{deep}} \tag{3}$$

Global NPP is assumed to be a function of the partial pressure of atmospheric CO_2 (p^{CO_2}) and the SAT deviation from preindustrial equilibrium,

$$f_{\mathrm{NPP}} = \varphi_{\mathrm{NPP}}(p_A^{\mathrm{CO_2}}, \Delta T) \tag{4}$$

The net flux of carbon into the ocean is proportional to the gas transfer velocity (k_g) and the CO_2 partial pressure difference between surface air and seawater:

$$f_O = k_g A_O \varepsilon (p_A^{\mathrm{CO_2}} - p_S^{\mathrm{CO_2}}) \tag{5}$$

where Ao is ocean surface area and eps a unit conversion factor.

The global average perturbation in surface water $\Delta p_S^{\mathrm{CO_2}}$ is a function of dissolved inorganic carbon (DIC) in the surface ocean at constant alkalinity (Joos et al., 1996), and SAT (Takahashi et al., 1993).

$$\Delta p_S^{\mathrm{CO_2}} = \psi(\Delta\mathrm{DIC})\,\chi(\Delta T) \tag{6}$$

ΔDIC and $p_A^{\mathrm{CO_2}}$ are related to model variables (cf. tables 1, 2),

$$\Delta\mathrm{DIC} = \frac{m_S}{H_{\mathrm{mix}} A_O \varrho M_{\mu\mathrm{mol}} 10^{-15}\mathrm{Gt/g}} \tag{7}$$

$$p_A^{\mathrm{CO_2}} = m_A \cdot \varepsilon \tag{8}$$

The carbon cycle equation set is closed by the specification of f_{decay} and f_{deep} (section 2.3), as well as ΔT, i.e., the coupling to the climate component (section 2.2).

2.2 Climate component

BernSCM simulates the deviation in global mean SAT from the preindustrial state. SAT is approximated by the temperature perturbation of the surface ocean ΔT, which is calculated from heat uptake by the budget equation

$$\frac{\mathrm{d}\Delta T}{\mathrm{d}t} c_S = f_O^H - f_{\mathrm{deep}}^H \tag{9}$$

where c_s is the heat capacity of the surface layer, f_O^H is ocean heat uptake, and f_{deep}^H is heat uptake by the deep ocean (and accounts for the bulk of the effective heat capacity of the ocean). Continental heat uptake is neglected due to the much higher ratio of heat conductivity to heat capacity of the ocean in comparison to the continent.

Geosci. Model Dev. Discuss., https://doi.org/10.5194/gmd-2017-233
Manuscript under review for journal Geosci. Model Dev.
Discussion started: 2 November 2017

Geoscientific Model Development Discussions
Open Access
EGU

f_O^H is taken to be proportional to RF (Forster et al., 2007) and the separation of SAT from radiative equilibrium ($\Delta T = \Delta T^{\mathrm{eq}}(RF)$; see table 2 for parameter definitions),

$$f_O^H = \mathrm{RF}\left(1 - \frac{\Delta T}{\Delta T^{\mathrm{eq}}}\right)\frac{A_O}{a_O} \tag{10}$$

This relation follows from the assumption that feedbacks are linear in ΔT (e.g., Hansen et al., 1984). ΔT^{eq} is given by

$$\Delta T^{\mathrm{eq}} = \mathrm{RF}\frac{\Delta T_{2\times}}{\mathrm{RF}_{2\times}} \tag{11}$$

where $\Delta T_{2\times}$ is climate sensitivity (defined as the equilibrium temperature change corresponding to twice the preindustrial CO_2 concentration). Climate sensitivy is an external parameter, as the model does not represent the processes determining equilibrium climate response. RF of CO_2 is calculated as (Myhre et al., 1998)

$$\mathrm{RF}_{\mathrm{CO_2}} = \ln\left(\frac{p_A^{\mathrm{CO_2}}}{p_{A0}^{\mathrm{CO_2}}}\right)\frac{\mathrm{RF}_{2\times}}{\ln(2)} \tag{12}$$

where $p_A^{\mathrm{CO_2}}$ is the preindustrial reference concentration of atmospheric CO_2, and $\mathrm{RF}_{2\times}$ is the RF at twice the preindustrial CO_2 concentration. RF of other GHGs, aerosols etc. can be parametrized in similar expressions involving GHG and pollutant emissions and concentrations (Prather et al., 2001). In the provided BernSCM code, non-CO_2 RF is treated as an exogenous boundary condition. Total RF is then

$$\mathrm{RF} = \mathrm{RF}_{\mathrm{CO_2}} + \mathrm{RF}_{\mathrm{nonCO_2}} \tag{13}$$

The calculation of f_{deep}^H (section 2.3) completes the climate model.

2.3 Impulse response model components

The response of a linear system to a time-dependent forcing f can be expressed by

$$m(t) = \int_{t_0}^{t} f(t')r(t-t')\,\mathrm{d}t' \tag{14}$$

where equilibrium is assumed for $t \leq t_0$. The function r is the system's impulse response function (IRF), as can be shown by evaluating the integral for a Dirac impulse ($f(t') = \delta(t')$). The IRF indicates the fraction remaining in the system at time t of a pulse input at a previous time t'. Because of linearity of the integral, any physically meaningful integrand f can be represented as a sequence of such impulses of varying size.

In BernSCM, an IRF is used to calculate the perturbation of heat and carbon in the mixed surface ocean layer (mixed layer IRF, (Joos and Bruno, 1996). For carbon,

$$m_S(t) = \int_{t_0}^{t} f_O(t')r_O(t-t')\,\mathrm{d}t', \tag{15}$$

Geosci. Model Dev. Discuss., https://doi.org/10.5194/gmd-2017-233
Manuscript under review for journal Geosci. Model Dev.
Discussion started: 2 November 2017

and similarly, for heat

$$\Delta T(t)\, c_S = \int_{t_0}^{t} f_O^H(t') r_O(t-t')\,\mathrm{d}t' \tag{16}$$

where the initial SAT deviation is zero. This approach has been shown to faithfully reproduce atmospheric CO_2 and SAT as simulated with the models from which the IRF is derived (Joos and Bruno, 1996). For temperature, the linear approach works since relatively small and homogeneous perturbations of ocean temperatures do not affect the circulation strongly and can be treated as a passive tracer (Hansen et al., 2010).

Equation (15) closes the ocean C budget equation (3), as can be seen by taking the derivative with respect to time (using $r(0) = 1$),

$$\frac{\mathrm{d}m_S}{\mathrm{d}t} = f_O(t) - \underbrace{\left(-\int_{t_0}^{t} f_O(t') \frac{\mathrm{d}r_O}{\mathrm{d}t}(t-t')\,\mathrm{d}t' \right)}_{f_{\mathrm{deep}}} \tag{17}$$

where f_{deep} is the flux to the deep ocean. Similarly, equation (16) closes the budget equation for ocean heat uptake (9).

Another IRF is used for the carbon m_L in living or dead biomass reservoirs of the terrestrial biosphere,

$$m_L(t) = \int_{t_0}^{t} f_{\mathrm{NPP}}(t') r_L(t-t')\,\mathrm{d}t' + m_L(t_0) \tag{18}$$

Again, equation (18) closes the budget equation for the land biosphere (2), as shown by the derivative with respect to time,

$$\frac{\mathrm{d}m_L}{\mathrm{d}t} = f_{\mathrm{NPP}}(t) - \underbrace{\left(-\int_{t_0}^{t} f_{\mathrm{NPP}}(t') \frac{\mathrm{d}r_L}{\mathrm{d}t}(t-t')\,\mathrm{d}t' \right)}_{f_{\mathrm{decay}}} \tag{19}$$

The time derivative of the land IRF is also known as the decay response function (e.g., Joos et al., 1996).

The above IRFs can be expressed as a sum of exponentials,

$$r(t) = a_\infty + \sum_k a_k e^{-t/\tau_k} \tag{20}$$

where the constant term a_∞ corresponds to an infinite decay timescale.

The ocean IRF contains a positive constant coefficient a_∞, indicating a fraction of the perturbation that will remain indefinitely (implied by carbon conversation in the ocean model). $CaCO_3$ compensation by sediment dissolution and weathering (Archer et al., 1998) are not considered here, but could be described using analogous elimination processes with time scales on the order of 10^4 to 10^5 kyr (Joos et al., 2004). In land biosphere models, in contrast, organic carbon is lost to the atmosphere by oxidation to CO_2 at non-zero rates, and consequently all timescales are finite (i.e., $a_\infty = 0$), and the IRF tends to zero (Figure 2).

Geosci. Model Dev. Discuss., https://doi.org/10.5194/gmd-2017-233
Manuscript under review for journal Geosci. Model Dev.
Discussion started: 2 November 2017

Geoscientific Model Development Discussions

Presently the parameters of the ocean mixed layer IRF are fixed. A possible change of ocean transport due to global warming is not captured. In contrast, the HRBM land biosphere IRF is temperature-dependent, and captures the enhancement of biomass decay by global warming (s.a. Table 3 and section 3).

Inserting formula (20) in the pulse response equation (14) yields

$$m(t) = \sum_k \int_0^t f(t')\, a_k e^{-(t-t')/\tau_k}\, \mathrm{d}t' \tag{21}$$

Thus the expression (14) separates into a set of independent integrals m_k corresponding to the number of time scales of the response. Taking the time derivative of expression (21) reveals the equivalence to a diagonal system of linear differential equations,

$$\begin{aligned} \frac{\mathrm{d}m_k}{\mathrm{d}t} &= f(t)\, a_k - m_k/\tau_k \\ m &= \sum_k m_k \end{aligned} \tag{22}$$

The direct numerical evaluation of the equation (14) involves integrating over all previous times at each timestep. The differential form (22) allows a recursive solution, which is much more efficient, especially for long simulations (the recursive solution implemented in BernSCM is described in appendix A).

Equation (22) shows the IRF to be equivalent to a box model, whereby each box m_k receives a fraction a_k of the input f, and has a characteristic turnover time τ_k (Figure 1). For the mixed ocean surface layer the carbon content of box k is given by:

$$\frac{\mathrm{d}m_{S_k}}{\mathrm{d}t} = f_O(t)\, a_{O_k} - m_{S_k}/\tau_{O_k} \tag{23}$$

and the change in total carbon content in the mixed layer is:

$$m_S = \sum_k m_{S_k} \tag{24}$$

Similar equations describe the heat content in the ocean surface layer, as well as the carbon stored in the land biosphere (Figure 1).

Thinking of IRF components as box models is conceptually meaningful. The simple Bern 4 box biosphere model (cf. table 3), for example, contains boxes corresponding to ground vegetation, wood, detritus, and soil. The HRBM land component, on the other hand, is abstractly defined by an IRF, but corresponds to boxes which correlate with biospheric reservoirs. However, since different box models may show a similar response, in practice the coefficients a_k and time scales τ_k may not be uniquely defined by the IRF, and should be interpreted primarily as abstract fitting parameters (Enting, 2007).

The timescales of an IRF describing a linear system may be thought of as the inverse eigenvalues of the model matrix of that system. For example, the timescales of the mixing layer IRF are the inverse eigenvalues of a matrix describing a diffusive multilayer ocean model (Hooss et al., 2001). A large model matrix yields a spectrum of many eigenvalues and timescales and corresponding model boxes. In practice, IRFs are approximated with fewer fitting parameters and, equivalently, timescales

Geosci. Model Dev. Discuss., https://doi.org/10.5194/gmd-2017-233
Manuscript under review for journal Geosci. Model Dev.
Discussion started: 2 November 2017

Geoscientific Model Development Discussions
Open Access
EGU

(4-6 in the case of BernSCM). Joos et al. (1996) used IRFs combined from two or more functions to minimize the number of parameters needed for an accurate representation. In BernSCM, simple IRFs of the form (20) are used exclusively. This allows adequate accuracy and a consistent interpretation as a multibox model.

3 Carbon cycle uncertainty assessment

The carbon cycle-climate uncertainty of simulations with BernSCM can be assessed in two ways. First, to assess structural uncertainty, different substitute models for the ocean and land components can be used (Table 3). Currently, this approach is quite limited by the set of available substitute models. Second, parameter uncertainty can be assessed by varying the temperature and CO_2 sensitivities of the model, based on a standard set of components that represent the key dependencies as completely as possible (here, the IRF substitutes for the HILDA ocean model, and the HRBM land biosphere model are used for the standard setup).

The uncertainties of the global carbon cycle concern the sensitivity of the modelled fluxes of carbon and heat to changing atmospheric CO_2 and climate. Key uncertainties strongly affecting the overall climate response are associated with land C storage: The dependency of NPP on CO_2 (CO_2 fertilization, eq. 4), and the dependency of land C on temperature (f_{decay} increases with warming, eq. (2)) give rise to large and opposed carbon fluxes which are both very uncertain in magnitude (Le Quéré et al., 2016). While all substitute land models available for BernSCM include CO_2 fertilization, only the HRBM substitute model represents temperature sensitivity of biomass decay (IRF parameters are temperature-dependent; Table 3).

As for the ocean, the uncertainty of heat uptake into the surface ocean is treated in terms of climate sensitivity (eq. 10). The efficiency of the uptake of heat (f^H_{deep}) and carbon (f_{deep}) into the deep ocean is not sensitive to temperature, as the currently available substitute models all represent a fixed circulation pattern (IRF parameters are not temperature dependent). The nonlinear chemistry of CO_2 dissolution in the surface ocean (eq. 5), which determines the sensitivity of ocean C uptake to atmospheric CO_2, is scientifically well established (Dickson et al., 2007; Orr and Epitalon, 2015), and is not treated as an uncertainty in BernSCM. The temperature sensitivities of NPP (eq. 4) and CO_2 dissolution in the surface ocean (eq. 6) are treated as uncertain here, but have secondary influence on the climate response.

Similar to previous studies using models from the Bern family (Plattner et al., 2008; Joos et al., 2001; Meehl et al., 2007; Van Vuuren et al., 2008), the parameter uncertainty range is assessed using the following setups:

"coupled": All temperature and CO_2 sensitivities at their standard values

"uncoupled": All sensitivities zero (except from the ocean CO_2 dissolution chemistry)

"Conly": Only CO_2 dependencies considered (CO_2 fertilization)

"Tonly": Only temperature dependencies considered (NPP, decay and ocean C uptake)

Climate models with explicit and detailed carbon cycle components exhibit a wide range of responses, as shown in the intercomparison studies of climate models with a detailed carbon cycle, C4MIP (Friedlingstein et al., 2006) and CMIP5 (Jones

Geosci. Model Dev. Discuss., https://doi.org/10.5194/gmd-2017-233
Manuscript under review for journal Geosci. Model Dev.
Discussion started: 2 November 2017

Geoscientific Model Development Discussions

et al., 2013). The authors analysed the feedback of carbon cycle-climate models using linearized sensitivity measures. These are derived from a simulation with temperature dependence ("coupled") and one without ("uncoupled"; note that these names have a different meaning in BernSCM). Total CO_2 emissions for the "coupled" (left hand side) and "uncoupled" (right hand side) simulations can be expressed as

$$\Delta C_A^c(\varepsilon+\beta_L+\beta_O+\alpha(\gamma_L+\gamma_O)) = \Delta C_A^u(\varepsilon+\beta_O+\beta_L) \tag{25}$$

where ΔC_A is the cumulative change in atmospheric CO_2 (in ppm) in the coupled (c) or uncoupled (u) case, and the terms in brackets represent the total sensitivity of C storage to ΔC_A; in particular, β is the change in carbon stored (in GtC) on land (L) or in the ocean (O) in response to atmospheric CO_2 change, γ is similarly the change in carbon storage in response to warming, and α is the transient climate sensitivity with respect to atmospheric CO_2 concentration; ε converts ppm to GtC (cf. Table 2; the formula in the original paper implies identical units for atmospheric and stored carbon).

The climate-carbon cycle feedback is measured by the feedback parameter g, defined by

$$\frac{\Delta C_A^c}{\Delta C_A^u} = \frac{1}{1-g} \tag{26}$$

and is thus estimated by

$$g = -\frac{\alpha(\gamma_L+\gamma_O)}{\varepsilon+\beta_O+\beta_L} \tag{27}$$

Thus the feedback strength scales with the assumed climate sensitivity and the temperature sensitivities, and is reduced by CO_2-induced sinks.

The BernSCM sensitivity setups can be expressed in terms of the C4MIP sensitivity parameters: Tonly corresponds to $\beta_L = 0$, Conly to $\gamma_L = \gamma_O = 0$, and uncoupled to $\beta_L = \gamma_L = \gamma_O = 0$. This can be used to estimate climate-carbon cycle feedback g captured in BernSCM. A comparison of the uncertainty ranges for BernSCM (including structural and parameter uncertainty) and the C4MIP ensemble is shown in section 4.

4 Illustrative simulations with BernSCM

In this section, simulations with BernSCM are compared with the results from two multi-model intercomparison projects: an analysis of Carbon dioxide and climate impulse response functions (Joos et al., 2013, here referred to as IRFMIP), and the C4MIP Climate–Carbon Cycle Feedback Analysis (Friedlingstein et al., 2006).

Coupled carbon cycle-climate models can be characterized and compared based on their response to a CO_2 emission pulse to the atmosphere (Joos et al., 2013). In IRFMIP, the airborne fraction (AF) for a pulse of 100 GtC, emitted on top of current (i.e., year 2010) atmospheric CO_2 concentrations, was simulated by a set of 15 carbon cycle-climate models of different complexity. For three of these models (Bern3D-LPJ, GENIE, MAGICC), ensembles sampling the parameter uncertainty of these models are included in IRFMIP. Thus, IRFMIP captures structural as well as parameter uncertainty.

The IRFMIP pulse experiment was repeated with BernSCM, exploring parameter uncertainty of the carbon cycle (section 3), as well as structural uncertainty, using the ocean model IRFs HILDA and Princeton in various combinations with the land

Geosci. Model Dev. Discuss., https://doi.org/10.5194/gmd-2017-233
Manuscript under review for journal Geosci. Model Dev.
Discussion started: 2 November 2017

biosphere components HRBM and Bern-4box (Figure. 3). Simulations were run for equilibrium climate sensitivities of 3°C (standard setup), 2 K, and 4.5 K.

The AF simulated with BernSCM broadly agrees with the set of simulations from IRFMIP. 100 years after the pulse, it is 0.30 (0.34–0.57) for a climate sensitivity of 3K (for coupled setup with uncertainty range in brackets). Climate sensitivity uncertainty only slightly affects the upper end of this range (Figure 3). For AF simulated with BernSCM, the standard coupled setup is close to the IRFMIP multimodel median, but the BernSCM uncertainty range is asymmetric. The IRFMIP multi-model range is similarly asymmetric. For the MAGICC and GENIE ensembles, the medians also correspond with the BernSCM standard case, while the uncertainty ranges are more symmetric, which may be related to the method used to sample the parameter uncertainties.

The BernSCM SAT response also broadly agrees with IRFMIP. The standard coupled simulation is somewhat lower than the IRFMIP median, which is explained in part by the climate sensitivity (3 K) being slightly lower than the IRFMIP average (3.2). The short term temperature response of BernSCM in particular is on the lower side of the IRFMIP range, suggesting stronger ocean mixing. The quickest initial temperature increase of the BernSCM simulations is obtained with the Princeton ocean model component (dashed lines), which shows a slower initial mixing to the deep ocean than the other implemented components (Figure 2). The comparability of the SAT projections is limited, as the range of climate sensitivities considered in the BernSCM simulations (2-4.5 K) differ somewhat from that of the IRFMIP multimodel set (1.5-4.6 K) and the single model ensembles (1.9-5.7 K), and are compounded with RF differences resulting from the uncertainty in atmospheric CO_2.

The C4MIP study used a SRES A2 emission scenario to compare the carbon cycle sensitivities of a range of models. As in the C4MIP exercise, BernSCM was run for SRES A2 without any non-CO_2 forcings (Figure 4; prescribed historical and scenario emissions were smoothed with the R smooth.spline function (R Core Team, 2015) for 41 degrees of freedom for use with different time steps). Land use was treated as an exogenous CO_2 emission, while the land model simulates an undisturbed biosphere.

The C4MIP results can be compared to the BernSCM simulations using the carbon cycle sensitivity parameters defined in section 3 (Table 4). The sensitivity parameters for the BernSCM standard simulation (HILDA-HRBM with coupled carbon cycle) lie within the C4MIP range. The uncertainty range for BernSCM, however, is not congruent with the multi-model range of C4MIP. Maximum and standard sensitivity for BernSCM are practically identical. Notably, this sensitivity is smaller (absolutely) than the C4MIP average for the land carbon response to CO_2 increase and warming. The resulting gain g is also smaller, though this results in large part from the lower climate sensitivity in BernSCM (which corresponds to 2.5 K as used for the Bern-CC model contribution to C4MIP). The lower end (in absolute terms) of the BernSCM carbon cycle sensitivity range is, on the other hand, zero per definition for all but the ocean-CO_2 sensitivity β_O (see section 3). As a consequence, the climate-carbon cycle feedback range also includes zero. In contrast, the C4MIP range does not include zero for all sensitivity parameters.

The land carbon uptake until 2100, under the different BernSCM configurations, varies over 500 GtC (Figure 4), more than three times the range of ocean uptake (180 GtC). This partly reflects the limited coverage of the uncertainty in ocean mixing,

Geosci. Model Dev. Discuss., https://doi.org/10.5194/gmd-2017-233
Manuscript under review for journal Geosci. Model Dev.
Discussion started: 2 November 2017

but also the fact that the land carbon sink is, together with the land use-related source, the most uncertain item in the budget (Le Quéré et al., 2009).

Together, the uncertainties in the carbon cycle sensitivities amount to a range of about 200 ppm in the projected atmospheric CO_2 for this scenario around 2100; the SAT range, after emissions have ceased in 2100, reaches roughly 1 K. Thus the carbon cycle uncertainty range amounts to about 1/3 of the total anthropogenic perturbation for both CO_2 and SAT.

5 Discussion

We simulated illustrative scenarios from two recent multi-model studies, C4MIP and IRFMIP, to compare BernSCM to the literature of carbon-cycle climate models. The results show that BernSCM is broadly representative of the current understanding of the global carbon cycle-climate response to anthropogenic forcing (in a time-averaged sense that does not address internal variability). The BernSCM uncertainty range in CO_2 and SAT projections is broadly similar to the ranges spanned by probabilistic single-model ensembles, and multi-model "ensembles of opportunity" such as the 15 IRFMIP models. The shown BernSCM uncertainty range consists mainly of parameter uncertainty and to a small extent of structural uncertainty. For the standard, coupled model setup, the sensitivities of ocean and land carbon uptake to changing CO_2 and climate (Table 4) of BernSCM are within the range of the detailed carbon cycle models in C4MIP. However, as some C4MIP models show much higher sensitivities, the BernSCM range does not capture the full C4MIP multi-model range. On the other hand, the C4MIP set is unlikely to sample uncertainty exhaustively, as each model contributed only a single, "most likely" simulation. Thus it does not include zero (or weak) sensitivities, whereas the BernSCM range does.

Figure 3 illustrates the importance of a systematic appraisal of uncertainty considering not only the "most likely" model setups, as the standard coupled response in CO_2 and SAT is near the lower end of the range, and may thus understate the impact. This is even more the case if the key processes are not implemented fully. For example, the early model version Bern-SAR, which was used for the Global Warming Potential (GWP) estimates in the IPCC second assessment report (Schimel et al., 1996) and more recently for integrated assessment (e.g. Hijioka et al., 2006), lacks temperature sensitivity of land carbon uptake (corresponding to the Conly setup) and coincides with the lower end of the BernSCM range.

As Figure 4 shows, solutions with different timesteps and numerical schemes as implemented in BernSCM are largely equivalent for a sufficiently smooth forcing. This offers the flexibility to opt for simplicity of implementation or maximum speed as required by the application (see also Appendix A).

Currently, a limited set of substitute models is available and included with BernSCM. The simple structure and open source policy of BernSCM allows users to address these current limitations according to the needs of their applications. More components can be added using the existing ones as a template. This requires the specification of the IRF and the parametrization of gas exchange for the surface ocean, or NPP for the land biosphere, respectively (as described in Joos et al., 1996; Meyer et al., 1999). For the ocean component, it is in principle possible to represent temperature dependency of ocean transport in the same way as it is done for the HRBM land biosphere component (Meyer et al., 1999), though this has not been done yet.

Geosci. Model Dev. Discuss., https://doi.org/10.5194/gmd-2017-233
Manuscript under review for journal Geosci. Model Dev.
Discussion started: 2 November 2017

One application of BernSCM is to use it as an emulator of the global long-term response of complex climate-carbon cycle models by adding the corresponding substitute model components. Additionally, pattern scaling can be applied to transfer the global mean temperature signal into spatially resolved changes in surface temperature, precipitation, cloud cover, etc., exploiting the correlation of global SAT with regional and local changes (Hooss et al., 2001). This allows to drive spatially explicit models, e.g., of terrestrial vegetation (as in Joos et al., 2001; Strassmann et al., 2008) or climate change-related impacts (as in Hijioka et al., 2009).

The addition of further alternative model components will extend the structural uncertainty that can be represented with BernSCM. A sufficient coverage of structural uncertainty could allow the interpolation between alternative model components, to represent uncertainty with scalable parameters (and removing the distinction between structural and parameter uncertainty). Such a parametrization of the uncertainty would enhance the possibilities for probabilistic applications of BernSCM.

6 Conclusions

BernSCM is a reduced-form carbon cycle-climate model that captures the characteristics of the natural carbon cycle and the climate system essential for simulating the global long term response to anthropogenic forcing. Simulated atmospheric CO_2 concentrations and SAT are in good agreement with results from two comprehensive multi-model ensembles. Process detail is minimal, due to the use of IRFs for system compartments that can be described linearly, and nonlinear parametrizations governing the carbon fluxes into these compartments. This framework allows, in particular, to represent the wide range of response time scales of the ocean and land biosphere, and the nonlinear chemistry of CO_2 uptake in the surface ocean - both essential for reliably simulating the global climate response to arbitrary forcing scenarios.

Due to its structural simplicitly and computational efficiency, BernSCM has many potential applications. In combination with pattern scaling, BernSCM can be used to project spatial fields of impact-relevant variables for applications such as climate change impact assessment, coupling with spatially explicit land biosphere models, etc. With alternative numerical solutions of varying complexity and stability to choose from, applications range from educational to computationally intensive integrated assessment modeling. BernSCM also offers a model-based alternative to GWPs for estimation of the climate impact of emissions and can be used to quantify climate benefits of mitigation options.

The generic implementation of linear IRF-components offers a transparent, extensible climate model framework. Current limitations concern the number of available substitute models (limiting the uncertainty range represented), and a fixed ocean transport. An addition of further alternative model components, and more flexible representation of sensitivities in terms of continuously variable parameters would further increase the models usefulness, for example for probabilistic applications.

Code availability. The source code of the Bern Simple Climate Model is available from the github repository at https://doi.org/10.5281/zenodo.1038117

Geosci. Model Dev. Discuss., https://doi.org/10.5194/gmd-2017-233
Manuscript under review for journal Geosci. Model Dev.
Discussion started: 2 November 2017

Geoscientific Model Development Discussions

Appendix A: Implementation of the pulse-response model

A1 Discretization

For the solution of the pulse-response equation (14), two discrete approximations are implemented, which both correspond to the differential equation system (22).

First, f can be taken as constant over a sufficiently short timestep $\Delta t = t_i - t_{i-1}$. This approximation yields the system

$$
\begin{aligned}
m_n &= m_{\infty n} + \sum_k m_{kn} \\
m_{kn} &= m_{kn-1}\, e^{-\Delta t/\tau_k} + A_k\, f_{n-\frac{1}{2}}\, \Delta t\, e^{-\Delta t/\tau_k} \\
m_{\infty n} &= m_{\infty n-1} + A_\infty\, f_{n-\frac{1}{2}}\, \Delta t
\end{aligned}
\tag{A1}
$$

where the subscript n indicates the state at time t_n, and $f_{n-\frac{1}{2}}$ is the value of f at midpoints between t_{n-1} and t_n.

Second, for longer timesteps, a better approximation is obtained by assuming linear variation of f over each time step. This yields

$$
\begin{aligned}
m_{kn} &= m_{kn-1}\, e^{-\Delta t/\tau_k} + \left(A_k\, f_{n-1} + B_k\, (f_n - f_{n-1})\right) \Delta t\, e^{-\Delta t/\tau_k} \\
m_{\infty n} &= m_{\infty n-1} + \left(A_\infty\, f_{n-1} + B_\infty\, (f_n - f_{n-1})\right) \Delta t
\end{aligned}
\tag{A2}
$$

The coefficients in the above equations are given by

$$
\begin{aligned}
A_k &= a_k \frac{\tau_k}{\Delta t} (e^{\Delta t/\tau_k} - 1) \\
A_\infty &= a_\infty \\
B_k &= a_k \frac{\tau_k}{\Delta t} \left(1 - \frac{\tau_k}{\Delta t}(1 - e^{-\Delta t/\tau_k})\right) e^{\Delta t/\tau_k} \\
B_\infty &= \frac{a_\infty}{2}
\end{aligned}
\tag{A3}
$$

In the following, equations (A1-A3) are derived.

We substitute t' by $t - x$ in equation (14) to get

$$
m(t) = \int_t^{t_0} f(t-x) r(x)\, \mathrm{d}x \tag{A4}
$$

Taking f to be constant over one time step,

$$
m(t_n) \simeq \sum_{i=1}^{n} f(t_n - t_{i-\frac{1}{2}}) \int_{t_{i-1}}^{t_i} r(x)\, \mathrm{d}x, \tag{A5}
$$

where the midpoint value $t_{i-\frac{1}{2}}$ is used for accuracy. The integral in (A5) can be evaluated explicitly, to define an adapted, discrete IRF R_i,

$$
R_i = 1/\Delta t \int_{t_{i-1}}^{t_i} r(x)\, \mathrm{d}x \tag{A6}
$$

Geosci. Model Dev. Discuss., https://doi.org/10.5194/gmd-2017-233
Manuscript under review for journal Geosci. Model Dev.
Discussion started: 2 November 2017

Geoscientific Model Development Discussions

where Δt is the length of the (constant) time step. Evaluating the integral using the pulse-response function (20) yields

$$R_i = A_\infty + \sum_k A_k e^{-t_i/\tau_k} \tag{A7}$$

This allows to write equation (A5) as

$$\begin{aligned} m_n &= m_{\infty n} + \sum_k m_{kn} \\ m_{\infty n} &= \sum_{i=1}^{n} \Delta t\, f_{n-i+\frac{1}{2}}\, A_\infty \\ m_{kn} &= \sum_{i=1}^{n} \Delta t\, f_{n-i+\frac{1}{2}}\, A_k e^{-t_i/\tau_k} \end{aligned} \tag{A8}$$

To derive a recursive expression from equation (A8), split sums,

$$\begin{aligned} m_{\infty n} &= \Delta t \left(f_{n-\frac{1}{2}}\, A_\infty + \sum_{i=2}^{n} f_{n-i+\frac{1}{2}}\, A_\infty \right) \\ m_{kn} &= \Delta t \left(f_{n-\frac{1}{2}}\, A_k e^{-t_1/\tau_k} + \sum_{i=2}^{n} f_{n-i+\frac{1}{2}}\, A_k e^{-t_i/\tau_k} \right) \end{aligned} \tag{A9}$$

and replace indices $i = j+1$, setting $t_0 = 0$, $t_1 = \Delta t$, $t_{j+1} = t_j + \Delta t$

$$\begin{aligned} m_{\infty n} &= \Delta t \left(f_{n-\frac{1}{2}}\, A_\infty + \sum_{j=1}^{n-1} f_{n-1-j+\frac{1}{2}}\, A_\infty \right) \\ m_{kn} &= \Delta t \left(f_{n-\frac{1}{2}}\, A_k e^{-\Delta t/\tau_k} + \sum_{j=1}^{n-1} f_{n-1-j+\frac{1}{2}}\, A_k e^{-(t_j+\Delta t)/\tau_k} \right) \end{aligned} \tag{A10}$$

comparison with equation (A8) yields the recursive differential system (A1).

Assuming now linear variation of f over each time step in equation (14),

$$m(t_n) \simeq \sum_{i=1}^{n} \int_{t_{i-1}}^{t_i} \left(f_{n-i} + (f_{n-i+1} - f_{n-i}) \frac{t_i - x}{\Delta t} \right) r(x)\, \mathrm{d}x, \tag{A11}$$

$$= \sum_{i=1}^{n} f_{n-i} \int_{t_{i-1}}^{t_i} r(x)\, \mathrm{d}x + (f_{n-i+1} - f_{n-i}) \int_{t_{i-1}}^{t_i} \left(\frac{t_i - x}{\Delta t} \right) r(x)\, \mathrm{d}x \tag{A12}$$

Substituting equation (A6) for the first integral and using partial integration on the second, one obtains

$$m(t_n) \simeq \sum_{i=1}^{n} \left(f_{n-i} \Delta t\, R_i + \frac{f_{n-i+1} - f_{n-i}}{\Delta t} \left(\int_{t_{i-1}}^{t_i} \int_{t_{i-1}}^{x} r(y)\, \mathrm{d}y\, \mathrm{d}x \right) \right) \tag{A13}$$

Geosci. Model Dev. Discuss., https://doi.org/10.5194/gmd-2017-233
Manuscript under review for journal Geosci. Model Dev.
Discussion started: 2 November 2017

Geoscientific Model Development Discussions

The double integral of the pulse-response function evaluates to

$$\int_{t_{i-1}}^{t_i}\int_{t_{i-1}}^{x} r(y)\,\mathrm{d}y\,\mathrm{d}x = \sum_k B_k\, e^{-t_i/\tau_k}\,\Delta t^2 \tag{A14}$$

By a similar procedure as for the constant flux approximation, the recursive formulation (A2) is obtained.

A2 Numerical schemes

For the solution of the BernSCM model equations, both explicit and implicit time stepping is implemented.

The stability requirement for the numerical solution depends on the equilibration time for the ocean surface CO_2 pressure $p_S^{CO_2}$. Due to the buffering of the carbonate chemistry, the CO_2 equilibration time is smaller than the gas diffusion time scale (~ 10yr) by a ratio given by the buffer factor. For undisturbed conditions (buffer factor $\simeq 10$) the equilibration time is about 1 yr. With increasing DIC, the buffer factor increases and the equilibration time shortens, making the equation system stiffer. Accordingly, when the model is solved explicitly with a time step of 1 yr, instability typically occurs after sustained carbon uptake by the ocean, which can occur in many realistic scenarios.

For the tested scenario range, the explicite solution is stable at a time step on the order of 0.1 yr, for which the piecewise constant approximation is accurate. For larger step size, an implicit solution is required to guarantee stability.

The piecewise constant approximation is adequate for time steps up to 1 yr, and the piecewise linear approximation for up to decadal time steps. An overview of the performance of three representative settings (set at compile time) for the C4MIP A2 scenario is given in Table A1.

The explicit solution is only implemented for the piecewise constant approximation (A1) and is obtained by approximating $f_{n-\frac{1}{2}}$ with f_{n-1}.

For the implicit solution, the piecewise constant (A1) or the piecewise linear approximation (A2), respectively, is solved for the quantities at t_n, approximating $f_{n-\frac{1}{2}}$ by f_n where applicable. Equations (A1,A2) are expressed in a common equation by substituting

$$m_{kn} = m_{kn-1}\, p_{mk} + f_n\, p_{fk} + f_{n-1}\, p_{fk}^{\mathrm{old}} \tag{A15}$$

with the following parameters for the piecewise constant approximation (A1),

$$\begin{aligned} p_{mk} &= e^{-\Delta t/\tau_k} \\ p_{fk} &= \Delta t A_k e^{-\Delta t/\tau_k} \\ p_{fk}^{\mathrm{old}} &= 0 \end{aligned} \tag{A16}$$

and for the piecewise linear approximation (A2),

$$\begin{aligned} p_{mk} &= e^{-\Delta t/\tau_k} \\ p_{fk} &= \Delta t B_k e^{-\Delta t/\tau_k} \\ p_{fk}^{\mathrm{old}} &= \Delta t (A_k - B_k) e^{-\Delta t/\tau_k} \end{aligned} \tag{A17}$$

Geosci. Model Dev. Discuss., https://doi.org/10.5194/gmd-2017-233
Manuscript under review for journal Geosci. Model Dev.
Discussion started: 2 November 2017

Geoscientific Model Development Discussions

In the following, the implicit solution for the piecewise constant discretization is derived. Here, the fully implicit scheme for land and ocean exchange is discussed, but for stability, it is only crucial to treat ocean uptake implicitly.

Consider first the equation system for carbon, assuming temperature to be known (or neglecting temperature dependence of model coefficients). Equation (A15) is applied to land carbon exchange for the constant approximation (A16),

$$\begin{aligned} m_{Ln} &= m_L^{c\Delta} + \Delta f_{\mathrm{NPP}} \sum_k p_{fk_L} \\ m_L^{c\Delta} &= \sum_k m_{Lkn-1} p_{mk_L} + f_{\mathrm{NPP}n-1} \sum_k p_{fk_L} \end{aligned} \tag{A18}$$

where $m_L^{c\Delta}$ is the land carbon stock obtained after one time step if NPP remained constant ("constant flux commitment"), and $\Delta f_{\mathrm{NPP}} = (f_{\mathrm{NPP}n} - f_{\mathrm{NPP}n-1})$ is the change in NPP over one time step.

For ocean carbon uptake,

$$\begin{aligned} m_{Sn} &= m_S^{c0} + f_{On} \sum_k p_{fk_O} \\ m_S^{c0} &= \sum_k m_{Skn-1} p_{mk_O} \end{aligned} \tag{A19}$$

where m_S^{c0} is the value of m_S after one time step if $f_{On} = 0$ ("zero-flux commitment").

To solve the implicit system, the nonlinear parametrizations need to be linearized around t_{n-1}. Linearizing ocean surface CO_2 pressure (6) and inserting in equation (5) yields

$$f_{On} \simeq k_g A_O (m_{An} - \varepsilon p_{S,n-1}^{\mathrm{CO_2}}) + k_g A_O \, \varepsilon \left. \frac{\mathrm{d}p_S^{\mathrm{CO_2}}}{\mathrm{d}m_S} \right|_{n-1} (m_{Sn-1} - m_{Sn}) \tag{A20}$$

where equations (7,8) were used. Similarly, NPP (4) is linearized,

$$\Delta f_{\mathrm{NPP}n} \simeq \left. \frac{\mathrm{d}f_{\mathrm{NPP}}}{\mathrm{d}m_A} \right|_{n-1} (m_{An} - m_{An-1}) \tag{A21}$$

using equation (8).

The system is completed with the discretized budget equation (1)

$$m_{An} = m_{An-1} + (e_{n-\frac{1}{2}} - f_{On})\Delta t - (m_{Ln} - m_{Ln-1}) \tag{A22}$$

Here, $e_{n-\frac{1}{2}}$ is assumed to be known (though this only applies to the "forward" solution for atmospheric CO_2 from emissions, solving for emissions from CO_2 is also implemented in the model code).

After calculating the "commited" values ${m_L^{c\Delta}}_n, {m_S^{c0}}_n$ from the model state at t_{n-1}, equations (A19) through (A22) are solved

$$\begin{aligned} \Delta f_{\mathrm{NPP}} = \frac{\left. \frac{\mathrm{d}f_{\mathrm{NPP}}}{\mathrm{d}m_A} \right|_{n-1}}{UV + W} \Bigg(& m_{Ln-1} - m_L^{c\Delta} + \Delta t \, e_{n-\frac{1}{2}} + \Delta t \, k_g A_O \Big(\varepsilon p_{S,n-1}^{\mathrm{CO_2}} - m_{An-1} \\ & + \varepsilon \left. \frac{\mathrm{d}p_S^{\mathrm{CO_2}}}{\mathrm{d}m_S} \right|_{n-1} \Big[m_S^{c0} - m_{Sn-1} + \sum_k p_{fk_O} \big(\frac{m_{Ln-1} - m_L^{c\Delta}}{\Delta t} + e_{n-\frac{1}{2}} \big) \Big] \Big) \Bigg) \end{aligned} \tag{A23}$$

Geosci. Model Dev. Discuss., https://doi.org/10.5194/gmd-2017-233
Manuscript under review for journal Geosci. Model Dev.
Discussion started: 2 November 2017

with the auxiliary variables

$$U = k_g A_O \varepsilon \frac{\mathrm{d}p_S^{\mathrm{CO_2}}}{\mathrm{d}m_S}\bigg|_{n-1} \sum_k p_{fk_O} + 1 \tag{A24}$$

$$V = \frac{\mathrm{d}f_{\mathrm{NPP}}}{\mathrm{d}m_A}\bigg|_{n-1} \sum_k p_{fk_L} + 1 \tag{A25}$$

$$W = \Delta t\, k_g A_O \tag{A26}$$

and, after inserting into equation (A18),

$$f_{O\,n} = \frac{k_g A_O}{U+W}\left(m_{An-1} - \varepsilon p_{S,n-1}^{\mathrm{CO_2}} - \varepsilon \frac{\mathrm{d}p_S^{\mathrm{CO_2}}}{\mathrm{d}m_S}\bigg|_{n-1} (m_S^{c0} - m_{Sn-1}) - (m_{Ln} - m_{Ln-1}) + \Delta t\, e_{n-\frac{1}{2}}\right) \tag{A27}$$

The remaining variables are then calculated using equations (A19) and (A22), whereby first the components $m_{k\,n}$ are calculated as in equation (A15) and then summed. Finally, the non-linear parametrisations (5,6) are recalculated with the updated model state.

The order of these equations matters, as the updated variables are successively inserted into the following equations. The land part is solved first, and can be substituted by an explicite step or a separate model, while keeping the ocean step implicit.

An implicit time step is also implemented for calculating SAT from RF (again, solving RF from SAT is also implemented but not discussed here). $\mathrm{RF}(t_n)$ can be assumed as known, as atmospheric $\mathrm{CO_2}$ is calculated first (i.e., no linearization necessary). Applying equation (A15) to temperature,

$$\Delta T_n c_S = \Delta T^{c\Delta} c_S + \Delta f_O^H \sum_k p_{fk_O}$$

$$\Delta T^{c\Delta} = \sum_k \Delta T_{kn-1} p_{mk_O} + f_{O\,n-1}^H / c_S \sum_k p_{fk_O} \tag{A28}$$

where $\Delta T^{c\Delta}$ is the "commited temperature" for constant heat flux to the ocean, and $\Delta f_O^H = f_{O\,n}^H - f_{O\,n-1}^H$ is the change in heat flux over one time step. Equations (11,10,A28) are solved for f_O^H,

$$f_{O\,n}^H = \frac{\mathrm{RF}_n - \frac{\mathrm{RF}_{2\times}}{\Delta T_{2\times}} \Delta T^{c\Delta} + f_{Hn-1} \sum_k p_{fk_O} \frac{\mathrm{RF}_{2\times}}{\Delta T_{2\times} c_S}}{\frac{\mathrm{RF}_{2\times}}{\Delta T_{2\times} c_S} \sum_k p_{fk_O} + a_O / A_O} \tag{A29}$$

Temperature change ΔT_n then follows from equation (A28).

The case of piecewise linear approximation (A17) differs from the piecewise constant one (A16) only in a non-zero contribution of f_{n-1} and a slightly different budget equation,

$$m_{An} = m_{An-1} + \left(e_{n-\frac{1}{2}} - \frac{f_{On} + f_{On}}{2}\right) \Delta t - (m_{Ln} - m_{Ln-1}) \tag{A30}$$

The first difference merely changes the calculation of "committed" changes, and only the second difference affects the solution of the implicit time step. In practice, however, this can be neglected without loss of accuracy, and thus equations (A23 – A27) and (A29) are also used to solve the piecewise linear system (while equation (A30) is used to close the budget).

Geosci. Model Dev. Discuss., https://doi.org/10.5194/gmd-2017-233
Manuscript under review for journal Geosci. Model Dev.
Discussion started: 2 November 2017

A3 Temperature dependent parameters

Temperature change in general affects the behavior of the ocean and land biosphere compartments, which are represented by IRFs. Thus, IRF coefficients can be temperature dependent, as it is the case with the HRBM substitute land biosphere model. In the above derivations, the change of temperature over one time step was not considered.

BernSCM updates any temperature-dependent model parameters by approximating the current temperature ΔT_n by the "committed" temperature $\Delta T^{c\Delta}$ as defined in equation (A28). Accuracy is further improved by substituting $\Delta T^{c\Delta}$ for ΔT_n in evaluating equation (A20) with temperature dependent parametrisations (6).

Competing interests. The authors declare that they have no conflict of interest.

Acknowledgements. This work received support by the Swiss National Science Foundation (#200020_172476).

References

Archer, D., Kheshgi, H., and Maier-Reimer, E.: Dynamics of fossil fuel CO2 neutralization by marine CaCO3, Global Biogeochemical Cycles, http://www.agu.org/pubs/crossref/1998/98GB00744.shtml, 1998.

Budyko, M.: The effect of solar radiation variations on the climate of the earth, Tellus, 21, 611–619, http://onlinelibrary.wiley.com/doi/10.1111/j.2153-3490.1969.tb00466.x/abstract, 1969.

Dickson, A. G., Sabine, C. L., and Christian, J. R.: Handbook of methods for the analysis of the various parameters of the carbon dioxide system in sea water, USDOE, 2007.

Enting, I., Wigley, T., Heimann, M., and Scientific, C.: Future emissions and concentrations of carbon dioxide: Key ocean/atmosphere/land analyses, Tech. Rep. 31, CSIRO, Div. of Atmos. Res., Melbourne, Victoria, Australia, http://62.225.2.55/files/meetings/workshops/other_meetings/application/pdf/enting_2001a.pdf, 1994.

Enting, I. G.: Laplace transform analysis of the carbon cycle, Environ. Model. Softw., 22, 1488–1497, https://doi.org/http://dx.doi.org/10.1016/j.envsoft.2006.06.018, 2007.

Forster, P. M. D. F., Ramaswamy, V., Artaxo, P., Berntsen, T., Betts, R. A., Fahey, D. W. D., Haywood, J., Lean, J., Lowe, D. C. D., Myhre, G., Nganga, J., Prinn, R., Raga, G., Schulz, M., and Dorland, R. V.: Chapter 2: Changes in Atmospheric Constituents and in Radiative Forcing, in: Climate Change 2007: The Physical Science Basis. Contribution of Working Group I to the Fourth Assessment Report of the Intergovernmental Panel on Climate Change, edited by Solomon, S., Qin, D., Manning, M., Chen, Z., Marquis, M., Averyt, K. B., Tignor, M., and Miller, H. L., Cambridge Univ. Press, United Kingdom and New York, NY, USA, http://www.ak-geomorphologie.de/data/Ipccreport_text_2.pdf, 2007.

Friedlingstein, P., Cox, P., Betts, R., Bopp, L., Von Bloh, W., Brovkin, V., Cadule, P., Doney, S., Eby, M., Fung, I., and Others: Climate – Carbon Cycle Feedback Analysis: Results from the C4MIP Model Intercomparison, Journal of Climate, 19, 3337–3353, http://journals.ametsoc.org/doi/abs/10.1175/JCLI3800.1, 2006.

Hansen, J., Lacis, A., Rind, D., and Russell, G.: Climate sensitivity: Analysis of feedback mechanisms, Geophysical Monograph, 29, http://www.agu.org/books/gm/v029/GM029p0130/GM029p0130.shtml, 1984.

Hansen, J., Ruedy, R., Sato, M., and Lo, K.: Global surface temperature change, Reviews of Geophysics, pp. 1–29, https://doi.org/10.1029/2010RG000345.1.INTRODUCTION, http://www.agu.org/pubs/crossref/2010/2010RG000345.shtml, 2010.

Heck, V., Donges, J. F., and Lucht, W.: Collateral transgression of planetary boundaries due to climate engineering by terrestrial carbon dioxide removal, Earth Syst. Dynam., pp. 783–796, https://doi.org/10.5194/esd-7-783-2016, 2016.

Hijioka, Y., Masui, T., Takahashi, K., Matsuoka Y., and Harasawa, H.: Development of a support tool for greenhouse gas emissions control policy to help mitigate the impact of global warming, Environmental Economics and Policy Studies, 7, 331–345, 2006.

Hijioka, Y., Takahashi, K., Hanasaki, N., Masutomi, Y., and Harasawa, H.: Comprehensive assessment of climate change impacts on Japan utilizing integrated assessment model, Association of International Research Initiatives for Environmental Studies (AIRIES), pp. 127–133, 2009.

Hooss, G., Voss, R., and Hasselmann, K.: A nonlinear impulse response model of the coupled carbon cycle-climate system (NICCS), Climate Dynamics, 18, 189–202, http://www.springerlink.com/index/8dbphjl18ch5lprx.pdf, 2001.

Jones, C., Robertson, E., Arora, V., Friedlingstein, P., Shevliakova, E., Bopp, L., Brovkin, V., Hajima, T., Kato, E., Kawamiya, M., Liddicoat, S., Lindsay, K., Reick, C. H., Roelandt, C., Segschneider, J., and Tjiputra, J.: Twenty-First-Century Compatible CO2 Emissions and

Airborne Fraction Simulated by CMIP5 Earth System Models under Four Representative Concentration Pathways, Journal of Climate, 26, 4398–4413, 2013.

Joos, F.: Modellierung der Verteilung von Spurenstoffen im Ozean und des globalen Kohlenstoffkreislaufes, Phd thesis, Universität Bern, 1992.

Joos, F. and Bruno, M.: Pulse response functions are cost-efficient tools to model the link between carbon emissions, atmospheric CO2 and global warming, Physics and Chemistry of the Earth, 21, 471–476, 1996.

Joos, F., Bruno, M., Fink, R., and Siegenthaler, U.: An efficient and accurate representation of complex oceanic and biospheric models of anthropogenic carbon uptake, Tellus B, 48, 397–417, http://onlinelibrary.wiley.com/doi/10.1034/j.1600-0889.1996.t01-2-00006.x/abstract, 1996.

Joos, F., Müller-Fürstenberger, G., and Stephan, G.: Correcting the carbon cycle representation: How important is it for the economics of climate change?, Environmental modeling and assessment, 4, 133–140, https://doi.org/doi:10.1023/A:1019004015342, http://www.springerlink.com/index/W371957V0UJ4L1U2.pdf, 1999.

Joos, F., Prentice, I. C., Sitch, S., Meyer, R., Hooss, G., Plattner, G.-k. G., Gerber, S., and Hasselmann, K.: Global warming feedbacks on terrestrial carbon uptake under the Intergovernmental Panel on Climate Change (IPCC) emission scenarios, Global Biogeochemical Cycles, 15, 891–908, http://www.climate.unibe.ch/~joos/papers/joos01gbc.pdf, 2001.

Joos, F., Gerber, S., and Prentice, I.: Transient simulations of Holocene atmospheric carbon dioxide and terrestrial carbon since the Last Glacial Maximum, Global Biogeochemical ..., 18, 1–18, https://doi.org/10.1029/2003GB002156, http://www.agu.org/pubs/crossref/2004/2003GB002156.shtml, 2004.

Joos, F., Roth, R., Fuglestvedt, J. S., Peters, G. P., Enting, I. G., von Bloh, W., Brovkin, V., Burke, E. J., Eby, M., Edwards, N. R., Friedrich, T., Frölicher, T. L., Halloran, P. R., Holden, P. B., Jones, C., Kleinen, T., Mackenzie, F., Matsumoto, K., Meinshausen, M., Plattner, G.-K., Reisinger, A., Segschneider, J., Shaffer, G., Steinacher, M., Strassmann, K., Tanaka, K., Timmermann, A., and Weaver, a. J.: Carbon dioxide and climate impulse response functions for the computation of greenhouse gas metrics: a multi-model analysis, Atmos. Chem. Phys., 12, 2793–2825, https://doi.org/10.5194/acp-13-2793-2013, http://www.atmos-chem-phys-discuss.net/12/19799/2012/, 2013.

Landry, J. S., Parrott, L., Price, D. T., Ramankutty, N., , and Matthews, H. D.: Modelling long-term impacts of mountain pine beetle outbreaks on merchantable biomass, ecosystem carbon, albedo, and radiative forcing, Biogeosciences, 13, 5277–5295, https://doi.org/10.5194/bg-13-5277-2016, 2016.

Le Quéré, C., Raupach, M. R., Canadell, J. G., Marland et al., G., Le Quéré et al., C., Marland, G., Bopp, L., Ciais, P., Conway, T. J., Doney, S. C., Feely, R. a., Foster, P., Friedlingstein, P., Gurney, K., Houghton, R. a., House, J. I., Huntingford, C., Levy, P. E., Lomas, M. R., Majkut, J., Metzl, N., Ometto, J. P., Peters, G. P., Prentice, I. C., Randerson, J. T., Running, S. W., Sarmiento, J. L., Schuster, U., Sitch, S., Takahashi, T., Viovy, N., van der Werf, G. R., and Woodward, F. I.: Trends in the sources and sinks of carbon dioxide, Nature Geoscience, 2, 831–836, https://doi.org/10.1038/ngeo689, http://www.nature.com/doifinder/10.1038/ngeo689, 2009.

Le Quéré, C., Andrew, R. M., Canadell, J. G., Sitch, S., Korsbakken, J. I., Peters, G. P., Manning, A. C., Boden, T. A., Tans, P. P., Houghton, R. A., et al.: Global carbon budget 2016, Earth System Science Data, 8, 605, 2016.

Levasseur, A., Cavalett, O., Fuglestvedt, J. S., Gasser, T., Johansson, D. J. A., Jørgensen, S. V., Raugei, M., Reisinger, A., Schivley, G., Strømman, A., Tanaka, K., and Cherubini, F.: Enhancing life cycle impact assessment from climate science: Review of recent findings and recommendations for application to LCA, Ecological Indicators, 71, 163–174, 2016.

Mathijssen, P. J. H., Kähkölä, N., Tuovinen, J.-P., Lohila, A., Minkkinen, K., Laurila, T., and Väliranta, M.: Lateral expansion and carbon exchange of a boreal peatland in Finland resulting in 7000 years of positive radiative forcing, Journal of Geophysical Research: Biogeosciences, 122, 562–577, https://doi.org/10.1002/2016jg003749, 2017.

Meehl, G. A., Stocker, T. F., Collins, W. D., Friedlingstein, P., Gaye, A. T., Gregory, J. M., Kitoh, A., Knutti, R., Murphy, J. M., Noda, A., Raper, S. C. B., Watterson, I. G., Weaver, A. J., and Zhao, Z.-C.: Chapter 10: Global Climate Projections, in: Climate Change 2007: The Physical Science Basis. Contribution of Working Group I to the Fourth Assessment Report of the Intergovernmental Panel on Climate Change, edited by Solomon, S., Qin, D., Manning, M., Chen, Z., Marquis, M., Averyt, K. B., Tignor, M., and Miller, H. L., Cambridge Univ. Press, United Kingdom and New York, NY, USA, 2007.

Meyer, R., Joos, F., Esser, G., Heimann, M., Hooss, G., Kohlmaier, G., Sauf, W., Voss, R., and Wittenberg, U.: The substitution of high-resolution terrestrial biosphere models and carbon sequestration in response to changing {CO_2} and climate, Global Biogeochemical Cycles, 13, 785–802, 1999.

Myhre, G., Highwood, E. J., Shine, K. P., and Stordal, F.: New estimates of radiative forcing due to well mixed greenhouse gases, Geophysical Research Letters, 25, 2715–2718, 1998.

Oeschger, H., Siegenthaler, U., Schotterer, U., and Gugelmann, a.: A box diffusion model to study the carbon dioxide exchange in nature, Tellus, 27, 168–192, https://doi.org/10.1111/j.2153-3490.1975.tb01671.x, http://tellusa.net/index.php/tellusa/article/view/9900, 1975.

Orr, J. C. and Epitalon, J. M.: Improved routines to model the ocean carbonate system: mocsy 2.0, Geosci. Model Dev., 8, 485–499, 2015.

Plattner, G.-K., Knutti, R., and Joos, F.: Long-term climate commitments projected with climate-carbon cycle models, ...of Climate, 21, 2721–2751, http://journals.ametsoc.org/doi/abs/10.1175/2007JCLI1905.1, 2008.

Prather, M., Ehhalt, D., Dentener, F., Derwent, R., Dlugokencky, E., Holland, E., Isaksen, I., Katima, J., Kirchhoff, V., Matson, P., Midgley, P., and Wang, M.: Atmospheric chemistry and greenhouse gases, in: Climate Change 2001: The Scientific Basis. Contribution of Working Group I to the Third Assessment Report of the {Intergovernmental Panel on Climate Change}, edited by Houghton, J. T., Ding, Y., Griggs, D. J., Noguer, M., van der Linden, P. J., Dai, X., Maskell, K., and Johnson, C. A., pp. 239–287, Cambridge University Press, Cambridge, United Kingdom and New York, NY, USA, 2001.

R Core Team: R: A Language and Environment for Statistical Computing, R Foundation for Statistical Computing, Vienna, Austria, https://www.R-project.org/, 2015.

Sarmiento, J., Orr, J., and Siegenthaler, U.: A perturbation simulation of CO2 uptake in an ocean general circulation model, Journal of Geophysical Research, 97, 3621–3645, https://doi.org/10.1029/91JC02849, http://www.agu.org/pubs/crossref/1992/91JC02849.shtml, 1992.

Schimel, D., Alves, D., Enting, I. G., Heimann, M., Joos, F., Raynaud, D., and Wigley, T. M. L.: CO2 and the carbon cycle, in: IPCC Second Scientific Assessment of Climate Change, edited by Houghton, J. T., pp. 76–86, Cambridge Univ. Press, New York, 1996.

Schultz, P. a. and Kasting, J. F.: Optimal reductions in CO2 emissions., Energy policy, 25, 491–500, http://www.ncbi.nlm.nih.gov/pubmed/11542949, 1997.

Sellers, W.: A global climatic model based on the energy balance of the earth-atmosphere system, Journal of Applied Meteorology, 8, 392–400, http://books.google.com/books?hl=en&lr=&id=lhzK1-woaiQC&oi=fnd&pg=PA125&dq=A+global+climatic+model+based+on+the+energy+balance+of+the+Earth-atmosphere+system&ots=Ok4KSho1Wl&sig=tbfTBm8r4JExSKZ4ZROK0kP43FY, 1969.

Siegenthaler, U. and Joos, F.: Use of a simple model for studying oceanic tracer distributions and the global carbon cycle, Tellus B, 44B, 186–207, http://onlinelibrary.wiley.com/doi/10.1034/j.1600-0889.1992.t01-2-00003.x/abstract, 1992.

Siegenthaler, U. and Oeschger, H.: Transient temperature changes due to increasing CO2 using simple models, Annals of Glaciology, 5, 153–159, 1984.

Stocker, T., Wright, D., and Mysak, L. A.: A zonally averaged, coupled ocean-atmosphere model for paleoclimate studies, Journal of Climate, http://www.climate.unibe.ch/~stocker/papers/stocker92jc.pdf, 1992.

Strassmann, K. M., Joos, F., and Fischer, G.: Simulating effects of land use changes on carbon fluxes: past contributions to atmospheric {CO_2} increases and future commitments due to losses of terrestrial sink capacity, Tellus B, https://doi.org/10.1111/j.1600-0889.2008.00340.x, 2008.

Takahashi, T., Olafsson, J., and Goddard, J.: Seasonal variation of CO2 and nutrients in the high-latitude surface oceans: a comparative study, Global Biogeochemical Cycles, 7, 843–878, http://www.agu.org/pubs/crossref/1993/93GB02263.shtml, 1993.

Van Vuuren, D. P., Meinshausen, M., Plattner, G.-K., Joos, F., Strassmann, K. M., Smith, S. J., Wigley, T. M. L., Raper, S. C. B., Riahi, K., de la Chesnaye, F., den Elzen, M. G. J., Fujino, J., Jiang, K., Nakicenovic, N., Paltsev, S., Reilly, J. M., Vuuren, D. P. V., and Elzen, M. G. J. D.: Temperature increase of 21st century mitigation scenarios, Proceedings of the National Academy of Sciences, 105, 15 258–15 262, https://doi.org/10.1073/pnas.0711129105, http://www.pnas.org/content/105/40/15258.abstract, 2008.

Vuuren, D. P. V., Lowe, J., Stehfest, E., Gohar, L., Hof, A. F., Hope, C., Warren, R., Meinshausen, M., and Plattner, G.-k.: How well do integrated assessment models simulate climate change?, Climatic Change, https://doi.org/10.1007/s10584-009-9764-2, 2009.

Geosci. Model Dev. Discuss., https://doi.org/10.5194/gmd-2017-233
Manuscript under review for journal Geosci. Model Dev.
Discussion started: 2 November 2017

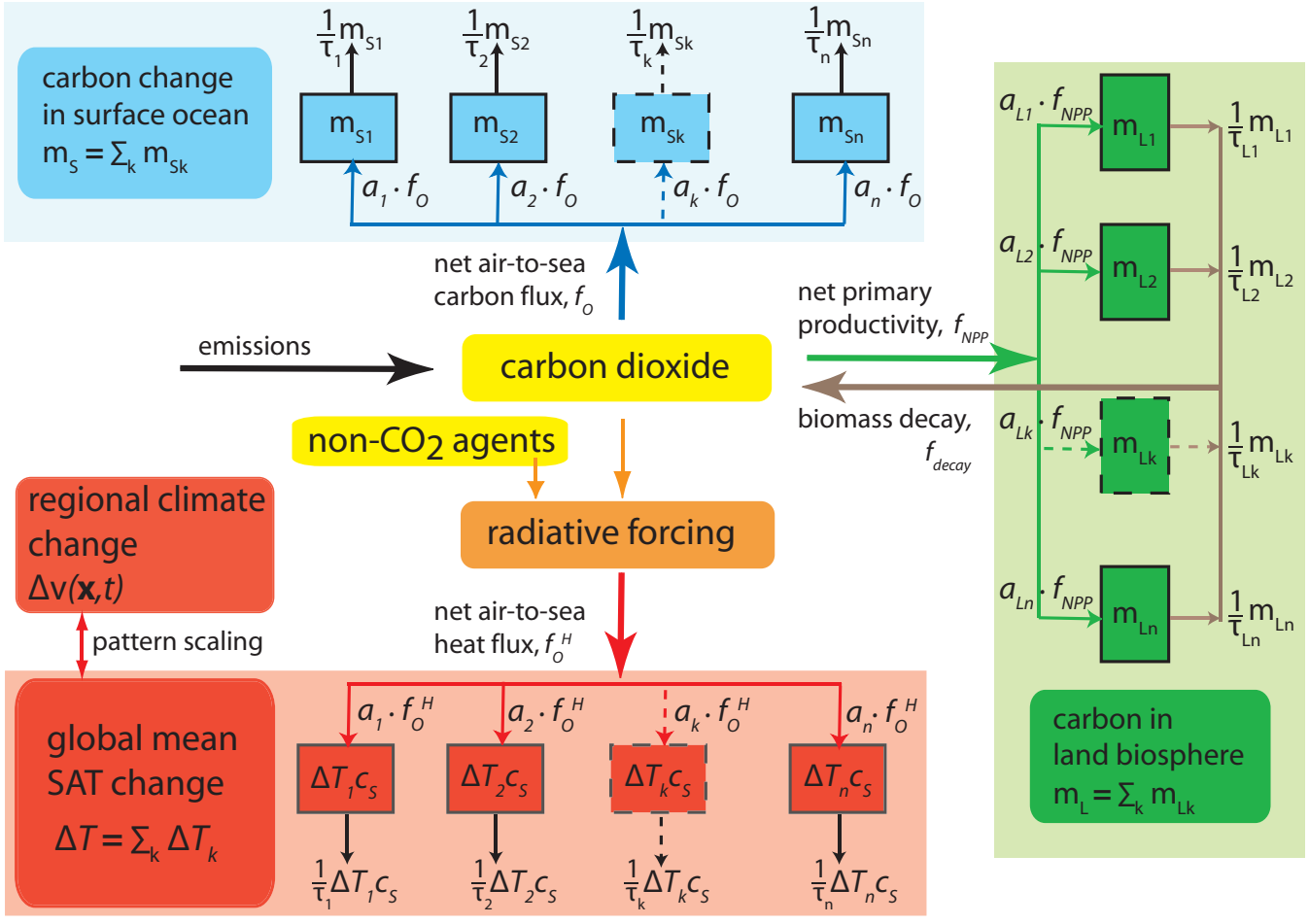

Figure 1. BernSCM as a box-type model of the carbon cycle-climate system based on impulse response functions. Heat and carbon taken up by the mixed ocean surface layer and the land biosphere, respectively, is allocated to a series of boxes with characteristic time scales for surface-to-deep ocean transport (τ) and of terrestrial carbon overturning (τ_L). The total perturbations in land and surface ocean carbon inventory and in surface temperature are the sums over the corresponding individual perturbations in each box, $(m_{Sk}, \Delta T_k, m_{Lk})$. Using pattern scaling, the response in SAT can be translated to regional climate change for fields $v(\mathbf{x},t)$ of variables such as SAT or precipitation.

Geosci. Model Dev. Discuss., https://doi.org/10.5194/gmd-2017-233
Manuscript under review for journal Geosci. Model Dev.
Discussion started: 2 November 2017

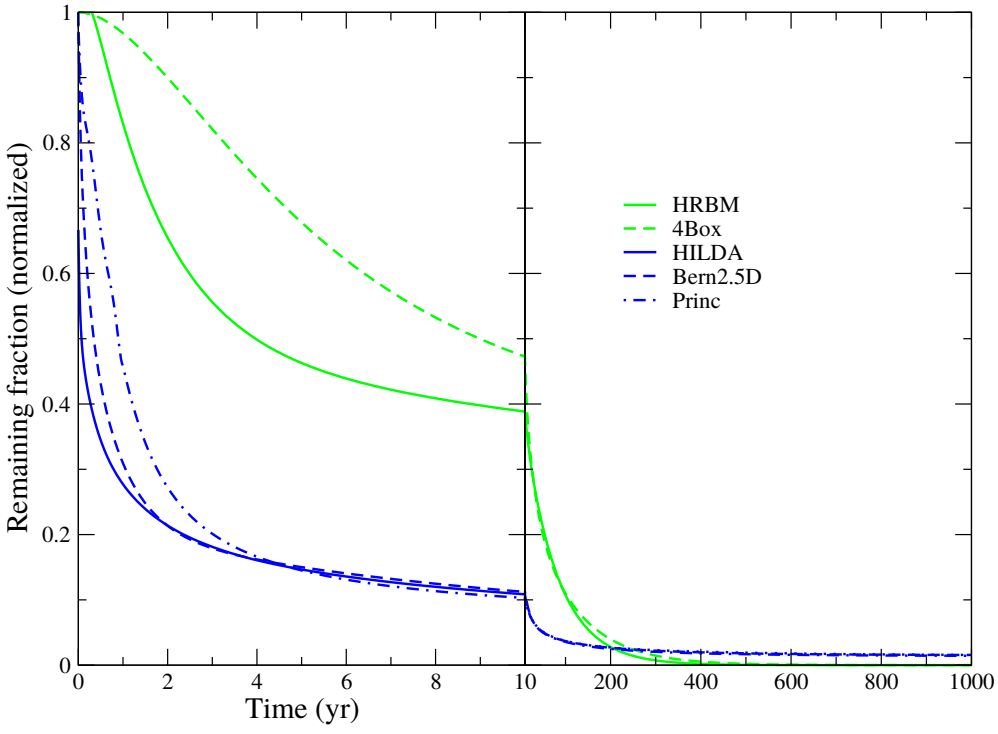

Figure 2. IRFs of ocean (blue) and land (green) model components (without temperature dependence). Ocean components are normalized to a common mixed layer depth of 50m (multiplied by H_{mix}/50m), causing initial response to deviate from 1.

Geosci. Model Dev. Discuss., https://doi.org/10.5194/gmd-2017-233
Manuscript under review for journal Geosci. Model Dev.
Discussion started: 2 November 2017

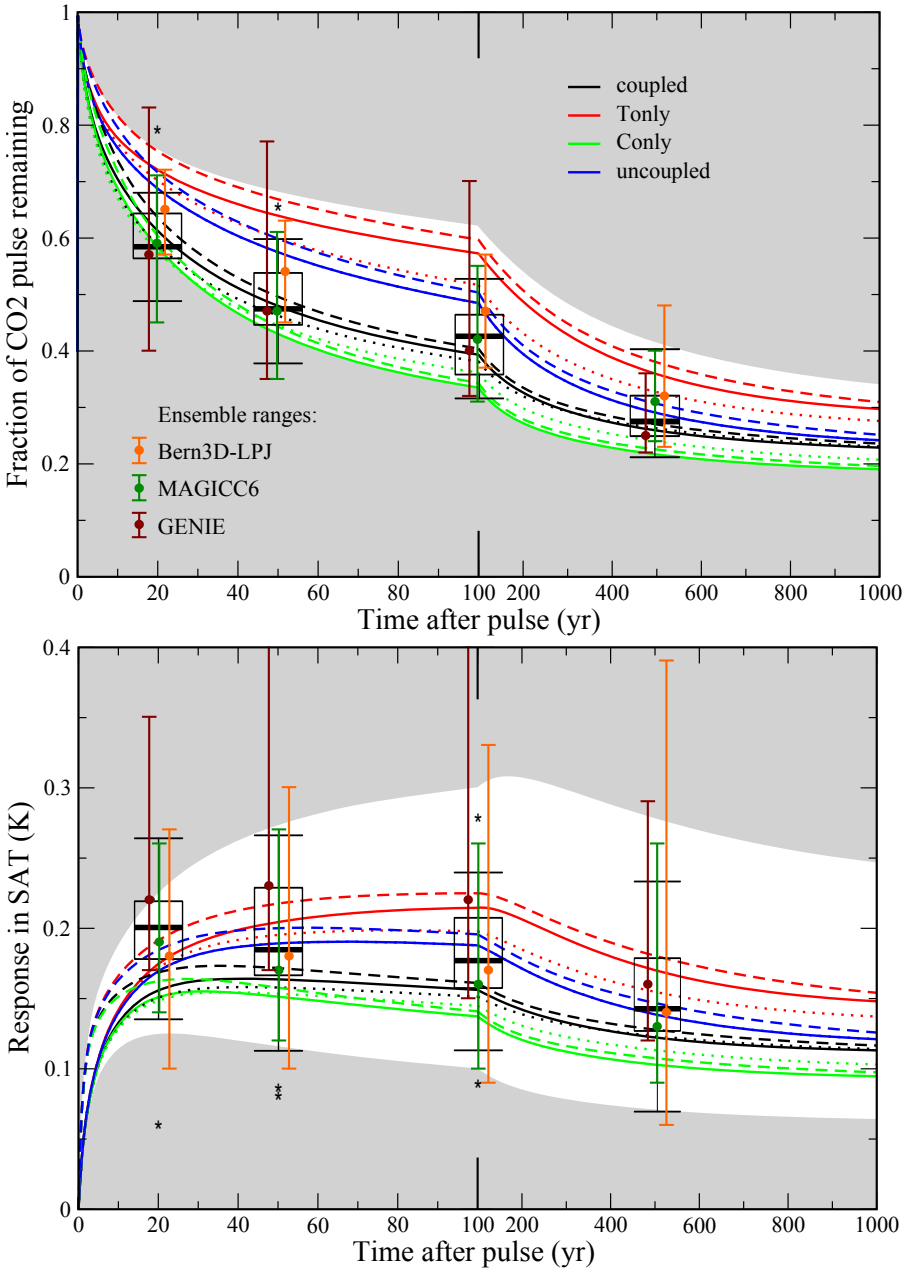

Figure 3. IRFMIP pulse response range compared to BernSCM range for parameter uncertainty (colors according to legend) and structural uncertainty, with model versions HILDA/HRBM (solid lines), HILDA/4box (dots), Princeton/HRBM (dashed). Standard climate sensitivity is 3 K, and a climate sensitivity range of 2–4.5 K is shown by the white area (envelope of all BernSCM runs). Single-model ensemble ranges from IRFMIP are included as errorbars indicating the 5-95% range and dots indicating the median. The multimodel IRFMIP range is shown by boxplots indicating median (bold black line), first quartiles (box), extreme values (whiskers) excluding outliers deviating from the median by more than 1.2 times the interquartile distance (asterisks).

Geosci. Model Dev. Discuss., https://doi.org/10.5194/gmd-2017-233
Manuscript under review for journal Geosci. Model Dev.
Discussion started: 2 November 2017

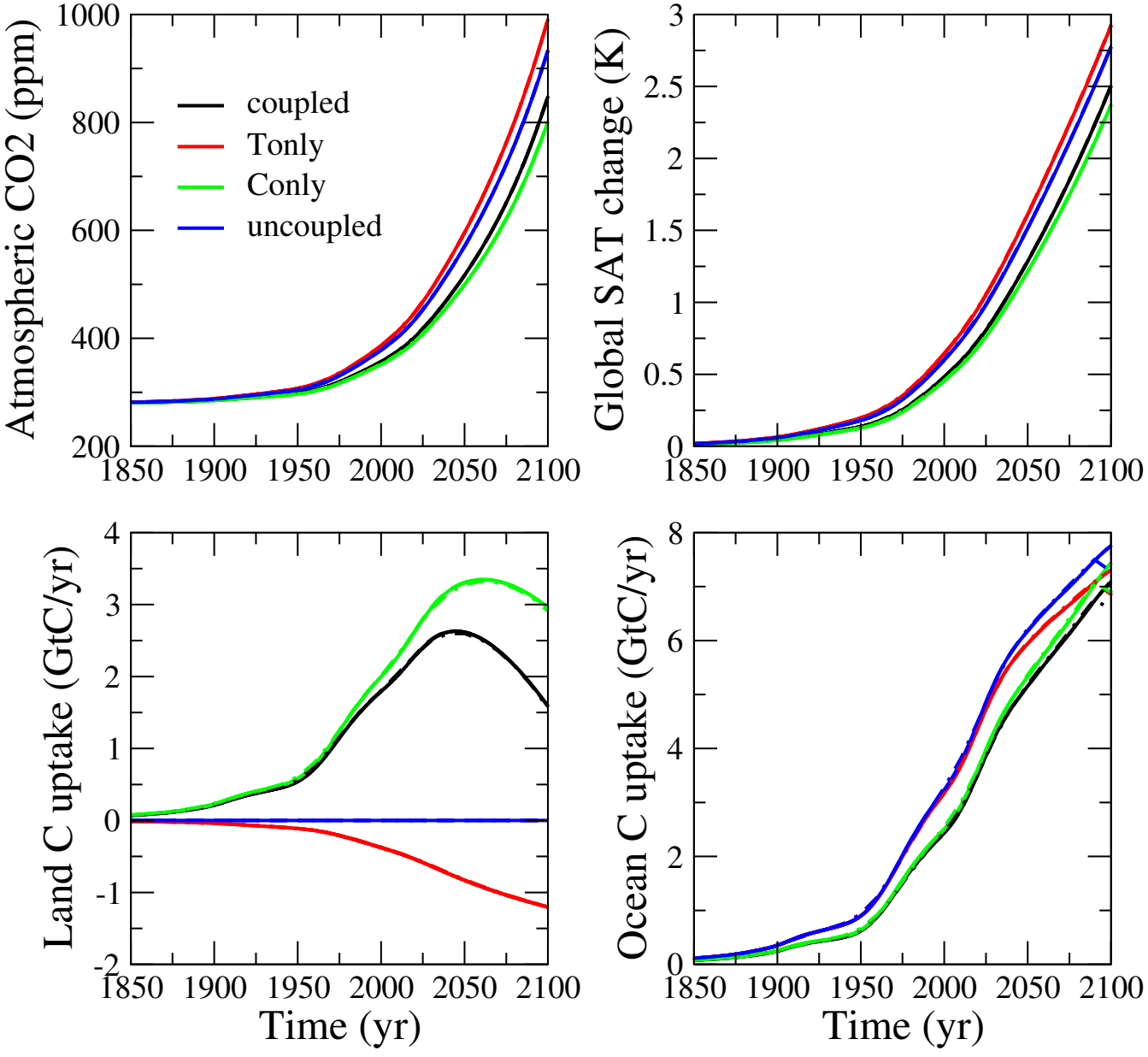

Figure 4. BernSCM simulations of the SRES A2 scenario used for C4MIP, with a climate sensitivity of 2.5°C and the HILDA/HRBM ocean/land components. Results for three numerical schemes are overlaid in the same line style; i. 0.1 yr Euler forward timestep (solid), ii. 1 yr implicit timestep (dashed), iii. 10 yr implicit timestep with piecewise linear approximation of fluxes (dash-dot); the difference at this resolution is only visible in C uptake.

Geosci. Model Dev. Discuss., https://doi.org/10.5194/gmd-2017-233
Manuscript under review for journal Geosci. Model Dev.
Discussion started: 2 November 2017

Geoscientific Model Development Discussions
Open Access
EGU

Table 1. Model variables

Variable	Meaning	Unit
m_A	atmospheric CO_2 carbon	GtC
m_L	land biomass carbon	GtC
m_O	ocean carbon perturbation	GtC
m_S	dissolved inorganic C perturbation in ocean mixed layer	GtC
ΔDIC	perturbation of dissolved inorganic C concentration in mixed layer	μmol/kg
$p_{A/S}^{CO_2}$	atmospheric/ocean surface CO_2 pressure	ppm
ΔT	global mean surface (ocean) temperature perturbation	K
e	CO_2 emissions	GtC/yr
f_A	net flux to atmosphere flux	GtC/yr
f_O	air-sea C flux	GtC/yr
f_{deep}	Flux mixed layer to deep	GtC/yr
f_{NPP}	NPP	GtC/yr
f_{decay}	decay of terrestrial biomass C	GtC/yr
f_O^H	air-sea heat flux	PetaW

Geosci. Model Dev. Discuss., https://doi.org/10.5194/gmd-2017-233
Manuscript under review for journal Geosci. Model Dev.
Discussion started: 2 November 2017

Geoscientific Model Development Discussions
Open Access
EGU

Table 2. Parameter definitions

Parameter	Meaning	Value
H_{mix}	depth of mixed ocean surface layer	50-75[a] m
A_O	Ocean surface area	$3.62 \cdot 10^{14}\mathrm{m}^2$
a_O	Ocean fraction of earth surface	0.71
ε	Atmospheric concentration per mass of C	2.123 ppm/GtC
ϱ	density of ocean water	1028 kg/m^3
c_p	heat capacity of water	4000 J/kg/K
c_s	mixed layer heat capacity	$c_p\,\varrho H_{\mathrm{mix}} A_O$
k_g	gas exchange coefficient	1/(9.06 yr$\cdot A_O$)
$M_{\mu\mathrm{mol}}$	micromol mass of DIC	$12.0107 \cdot 10^{-6}$ g
$\mathrm{RF}_{2\times}$	RF per doubling of atm. CO_2	3.708 Wm^{-2}

[a]Range for included ocean components

Geosci. Model Dev. Discuss., https://doi.org/10.5194/gmd-2017-233
Manuscript under review for journal Geosci. Model Dev.
Discussion started: 2 November 2017

Geoscientific Model Development Discussions
Open Access
EGU

Table 3. IRF substitute model components currently implemented in BernSCM, and the corresponding implemented dependencies on atmospheric CO_2 and SAT (references for the parametrisations used are given in the footnotes).

Ocean substitute model	Ocean C dependent on:
HILDA Joos (1992)	CO_2[a], SAT[b]
Princeton GCM Sarmiento et al. (1992)	
Bern2.5D Stocker et al. (1992)	
Land substitute model	**Land C dependent on:**
4box Siegenthaler and Joos (1992)	CO_2[c]
HRBM Meyer et al. (1999)	CO_2, SAT[d]

[a] Joos and Bruno (1996)
[b] Takahashi et al. (1993)
[c] Enting et al. (1994); Schimel et al. (1996)
[d] Meyer et al. (1999)

Geosci. Model Dev. Discuss., https://doi.org/10.5194/gmd-2017-233
Manuscript under review for journal Geosci. Model Dev.
Discussion started: 2 November 2017

Geoscientific Model Development Discussions
Open Access
EGU

Table 4. C4MIP sensitivity parameters. The BernSCM range covers the carbon cycle settings as discussed in section 3, and different combinations of model components (HILDA-HRBM, HILDA-4box, Princeton-HRBM); the C4MIP range covers all participating models.

	α	β_L	β_O	γ_L	γ_O	g
Unit	$10^{-3}\frac{\mathrm{K}}{\mathrm{ppm}}$	$\frac{\mathrm{GtC}}{\mathrm{ppm}}$	$\frac{\mathrm{GtC}}{\mathrm{ppm}}$	$\frac{\mathrm{GtC}}{\mathrm{K}}$	$\frac{\mathrm{GtC}}{\mathrm{K}}$	10^{-2}
			BernSCM			
Standard	4.4	0.75	1.2	-46	-31	8.3
Range	4.1–4.6	**0**–0.75	1.0–1.2	-46–**0**	-31–**0**	0–8.4
			C4MIP ensemble			
Average	6.1	1.35	1.13	-79	-30	15
Range	3.8–8.2	0.2–2.8	0.8–1.6	-177– -20	-67– -14	4–31

Geosci. Model Dev. Discuss., https://doi.org/10.5194/gmd-2017-233
Manuscript under review for journal Geosci. Model Dev.
Discussion started: 2 November 2017

Geoscientific Model Development Discussions
Open Access
EGU

Table A1. Performance and accuracy for time steps 1–10 yr relative to a reference with a time step of 0.1 yr. The reference simulation is solved explicitly, otherwise an implicit solution was used. The average execution time of the time integration loop is given as a fraction of the explicit case. For atmospheric CO_2 and SAT, the root mean square difference to the explicite case, divided by the value range over the simulation is given. All values are for the C4MIP A2 scenario (years 1700 – 2100), using the HILDA ocean component and the HRBM land component with standard temperature and carbon cycle sensitivities (coupled).

Δt	1yr	10yr
discretization	piecewise const.	piecewise lin.
execution time	15%	2 %
CO2 RMS/range	0.31‰	0.45‰
SAT RMS/range	0.52‰	0.53‰